New Mexico Geological Society

Downloaded from: https://nmgs.nmt.edu/publications/guidebooks/41



Proterozoic tectonic evolution of the Cimarron Mountains, north-central New Mexico

Jeffrey A. Grambling and R. D. Dallmeyer
1990, pp. 161-170. https://doi.org/10.56577/FFC-41.161

in:

Tectonic Development of the Southern Sangre de Cristo Mountains, New Mexico, Bauer, P. W.; Lucas, S. G.; Mawer, C. K.; McIntosh, W. C.; [eds.], New Mexico Geological Society 41st Annual Fall Field Conference Guidebook, 450 p. https://doi.org/10.56577/FFC-41

This is one of many related papers that were included in the 1990 NMGS Fall Field Conference Guidebook.

Annual NMGS Fall Field Conference Guidebooks

Every fall since 1950, the New Mexico Geological Society (NMGS) has held an annual Fall Field Conference that explores some region of New Mexico (or surrounding states). Always well attended, these conferences provide a guidebook to participants. Besides detailed road logs, the guidebooks contain many well written, edited, and peer-reviewed geoscience papers. These books have set the national standard for geologic guidebooks and are an essential geologic reference for anyone working in or around New Mexico.

Free Downloads

NMGS has decided to make peer-reviewed papers from our Fall Field Conference guidebooks available for free download. This is in keeping with our mission of promoting interest, research, and cooperation regarding geology in New Mexico. However, guidebook sales represent a significant proportion of our operating budget. Therefore, only *research papers* are available for download. *Road logs*, *mini-papers*, and other selected content are available only in print for recent guidebooks.

Copyright Information

Publications of the New Mexico Geological Society, printed and electronic, are protected by the copyright laws of the United States. No material from the NMGS website, or printed and electronic publications, may be reprinted or redistributed without NMGS permission. Contact us for permission to reprint portions of any of our publications.

One printed copy of any materials from the NMGS website or our print and electronic publications may be made for individual use without our permission. Teachers and students may make unlimited copies for educational use. Any other use of these materials requires explicit permission.

This page is intentionally left blank to maintain order of facing pages.

PROTEROZOIC TECTONIC EVOLUTION OF THE CIMARRON MOUNTAINS, NORTH-CENTRAL NEW MEXICO

JEFFREY A. GRAMBLING[1] and R. D. DALLMEYER[2]
[1]Department of Geology, University of New Mexico, Albuquerque, New Mexico 87131; [2]Department of Geology, University of Georgia, Athens, Georgia 30602

Abstract—The Cimarron Mountains contain three Proterozoic crustal blocks separated by ductile shear zones. The first block consists of greenschist-facies volcanic and plutonic rocks metamorphosed below 450°C; the second, amphibolite-facies quartzite metamorphosed at 500–550°C, 3.5–4.5 kb; and the third, granulite-facies supracrustal and plutonic gneisses metamorphosed at 800–850°C, 7.5–8.5 kb. The three crustal blocks were juxtaposed along two shear zones of different geometry and age. The older ductile shear zone, subhorizontal with top-to-the-southwest movement, separates underlying granulites from overlying amphibolite-facies quartzite. The underlying crustal block records a retrograde P-T path of cooling and decompression that intersects the peak metamorphic conditions of the overlying crustal block. Intersection of the P-T paths accompanied joining of the two crustal blocks across a synmetamorphic, mid-crustal extensional fault at 1400 Ma, as dated by $^{40}Ar/^{39}Ar$ analyses of hornblende. The younger ductile shear zone, nearly vertical and trending northwest, records right-slip ductile movement overprinted by much younger, brittle, vertical faulting. The early ductile movement juxtaposed greenschists against granulites, at P-T conditions in the greenschist facies. A muscovite $^{40}Ar/^{39}Ar$ spectrum may date this event at between 1295 Ma and 1100 Ma.

INTRODUCTION

The Cimarron Mountains form a large uplift east of the Moreno Valley in northern New Mexico (cf. Mawer et al., 1990; Fig. 1). Proterozoic rocks exposed east and southeast of Eagle Nest Lake were mapped by Wobus (1989), who reported several features that prompted us to begin a detailed study of the region. This paper presents our initial results. We document that basement rocks of the Cimarron Mountains belong to three Proterozoic tectonic blocks separated by ductile shear zones (see inset, Fig. 1). Differences in metamorphic grade require offset on these shear zones to be substantial.

The three tectonic blocks are assigned names to simplify discussion. The *Cimarron River tectonic block,* in the northeastern corner of Figure 1, contains plutonic and supracrustal rocks, the latter recording regional metamorphism in the middle to upper greenschist facies. The Fowler Pass fault, which bounds the southwestern margin of this block, is a steeply dipping, right-slip, Proterozoic ductile shear zone overprinted by much younger vertical movement. Granulite-facies gneiss dominates the *Eagle Nest tectonic block* southwest of the Fowler Pass fault. The granulites are overlain by an approximately horizontal ductile shear zone that separates them from overlying rocks of the *Tolby Meadow tectonic block*. The Tolby Meadow tectonic block consists largely of quartzite metamorphosed in the lower amphibolite facies. This paper describes rocks from the three Proterozoic crustal blocks, discusses their metamorphic and tectonic histories and provides a preliminary interpretation of how and when they were assembled.

METHODS

The area was mapped at 1:12,000 in 1988 and 1989. Mineral analyses were obtained with a JEOL 733 electron microprobe at the University of New Mexico following procedures described in Grambling et al. (1989) and Williams and Grambling (1990). All minerals were also subjected to 100-second energy-dispersive scans to look for elements not analyzed in the wavelength-dispersive mode; none were found.

Metamorphic conditions in the Cimarron River tectonic block were determined by comparing mafic mineral assemblages to the experimental studies of Moody et al. (1983) and Apted and Liou (1983). P-T measurements from the Eagle Nest tectonic block come from garnet-biotite (Hackler and Wood, 1989, Fe-Mg mixing in garnet; Ganguly and Saxena, 1984, Ca mixing in garnet; Williams and Grambling, 1990, Mn mixing in garnet and ferric iron in biotite) coupled with garnet-plagioclase-sillimanite-quartz barometry (Newton and Haselton, 1981; Koziol and Newton, 1988). Metamorphic conditions in the Tolby Meadow tectonic block were estimated from the assemblage sillimanite-chloritoid and the experiments of Holdaway (1971) and Rao and Johannes (1979).

Techniques used for $^{40}Ar/^{39}Ar$ analysis followed those of Dallmeyer and Keppie (1987). Optically pure (>99%) mineral concentrates were wrapped in aluminum foil packets, sealed in quartz vials and irradiated in either the U.S. Geological Survey TRIGA reactor or the H-5 position of the Ford Reactor at the University of Michigan. Variations in neutron flux along the length of the irradiation assembly were monitored with several mineral standards including MMhb-1 (Alexander et al., 1978). Samples were heated incrementally until fusion in a double-vacuum, resistance-heated furnace. Temperatures, monitored with a direct-contact thermocouple, were controlled to ±1°C between increments and are accurate to ±5°C. Blank-corrected isotopic ratios were adjusted for the effects of mass discrimination and interferring isotopes produced during irradiation using factors reported in Dalrymple et al. (1981; TRIGA reactor) or Harrison and FitzGerald (1986; Ford Reactor). Apparent $^{40}Ar/^{39}Ar$ ages were calculated from the corrected isotopic ratios using decay constants and abundance ratios in Steiger and Jager (1977). Intralaboratory uncertainties have been calculated by statistical propagation of uncertainties in measurement of each isotope ratio (at two standard deviations of the mean) through the age equation. Interlaboratory uncertainties are approximately ±1.25–1.5% of quoted ages.

Analysis of the MMhb-1 monitor indicates that apparent K/Ca ratios may be calculated through the relationship $0.505(\pm 0.003) \times (^{39}Ar/^{37}Ar)$ corrected (Ford Reactor) or $0.518(\pm 0.005) \times (^{39}Ar/^{37}Ar)$ corrected (TRIGA reactor). Analyses of amphibole concentrates were plotted on $^{36}Ar/^{40}Ar$ vs. $^{39}Ar/^{40}Ar$ isotope correlation diagrams using the regression techniques of York (1969). Total-gas ages were computed for each sample by appropriate weighting of the age and percent ^{39}Ar released within each temperature increment. A "plateau" is considered to be defined if the ages recorded by two or more contiguous gas fractions, with similar apparent K/Ca ratios, each representing more than 4% of the total ^{39}Ar evolved and together constituting >50% of the total quantity of ^{39}Ar evolved, agree within ±1%.

ROCK TYPES

Cimarron River tectonic block

Felsic volcanic rocks dominate the southwestern part of this tectonic block (Fig. 2) and contain quartz-plagioclase-K-feldspar-muscovite ± chlorite. Abundant relict quartz phenocrysts 1–3 mm across in a finer-grained matrix attest to the volcanic origin of this unit (Wobus, 1989). Rocks generally have only a weak foliation defined by sericite

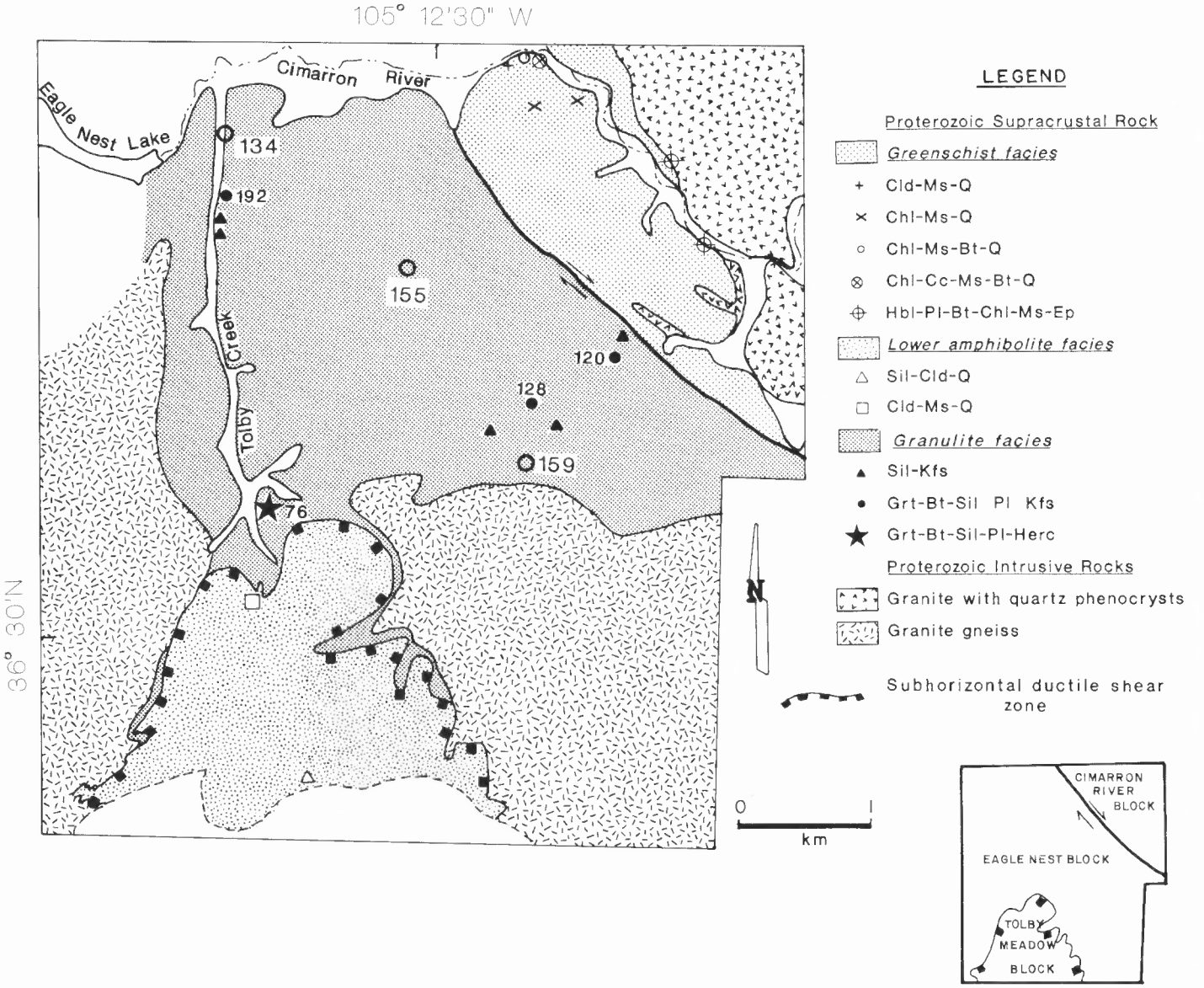


FIGURE 1. Simplified geologic map of Cimarron Mountains showing locations of mineral assemblages used to constrain metamorphic P-T conditions. Greenschist-facies rocks northeast of Fowler Pass fault form Cimarron River tectonic block; granulite facies rocks locally retrograded to amphibolite facies, southeast of Fowler Pass fault, define Eagle Nest tectonic block; and lower-amphibolite facies quartzite in south-central part of area make up Tolby Meadow tectonic block.

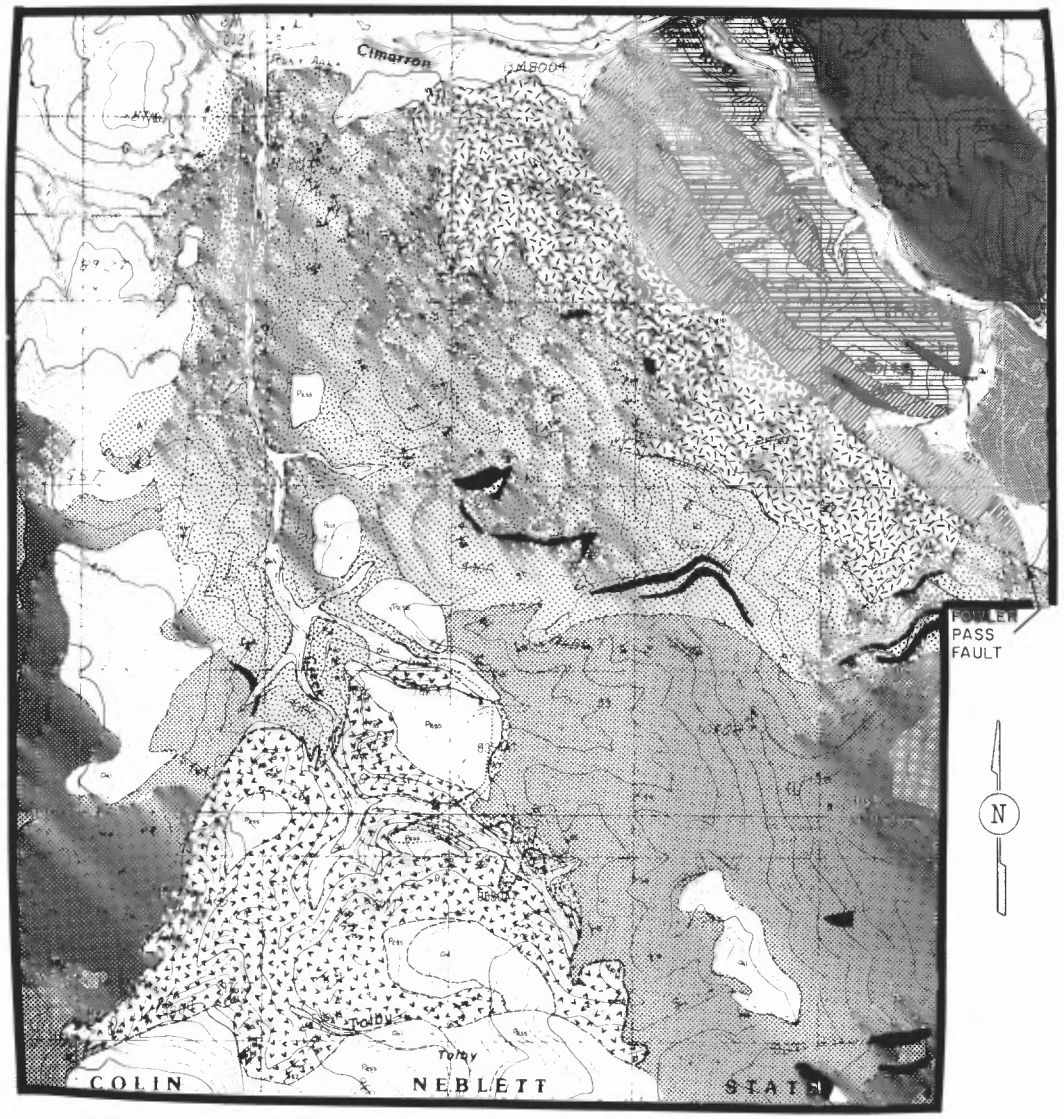
and chlorite except near the Fowler Pass fault, where foliation and lineation become dominant fabrics.

Thin layers of banded ironstone crop out within the felsic volcanic rocks. The ironstones have finely interbedded quartz-rich and iron-oxide-rich layers, with dominant oxide minerals being magnetite and hematite. They presumably formed as banded cherts. Although outcrops are too small to show in Figure 2, one is found south of the Cimarron River near 9000 ft elevation, immediately northeast of the Fowler Pass fault. Another, adjacent to the Horseshoe mine (Fig. 2), may have been the exploration target at the mine.

Foliated mafic metavolcanic rocks form a volumetrically important part of the Cimarron River tectonic block. They contain magnesian chlorite and albite with accessory titanite, FeTi oxide minerals and epidote. Most minerals have grain sizes below 0.1 mm, although relict volcanic plagioclase and some chlorites are larger. Chlorite makes up 60–80% of the mode. Veins of secondary quartz cut across some outcrops, and locally the rocks contain rounded segregations of quartz, 1–5 mm in diameter, that may have been vesicles. Mineralogy and grain size change dramatically within 50 m of the coarse-grained granitic pluton shown in Figure 2, where contact metamorphism resulted in development of the assemblage hornblende-biotite-Mg-rich chlorite-epidote-plagioclase-quartz-FeTi oxides. Minerals in the contact aureole average 1–5 mm in size and rocks preserve hornfelsic textures.

Pelitic metasedimentary beds too thin to show in Figure 2 are interbedded with both mafic and felsic rocks. The fine-grained, well-foliated pelites typically contain chlorite-muscovite-biotite-quartz, locally with calcite, epidote, titanite and feldspar. One specimen of aluminous pelite collected near the Horseshoe mine (Fig. 2) contains chloritoid, muscovite and quartz.

A pluton of coarse-grained granitic rock cuts across other contacts in the Cimarron River tectonic block (Figs. 1, 2). Wobus (1989) reported the pluton to have granitic to granodioritic composition. It contains ovoid phenocrysts of strained quartz typically 1 cm across but rarely up to 3 cm across, in a matrix of slightly finer-grained quartz-plagioclase-K-feldspar. The granite lacks a pervasive foliation. Several thin sills that extend along foliation, away from the main pluton into adjacent country rock, are texturally identical to the main granite, including lack of foliation. They may have intruded along pre-existing foliation; if so, the granite may have been emplaced after the regional penetrative deformation.



LEGEND

Phanerozoic rocks undivided (includes Quaternary alluvium and sandstone of unknown age)

Precambrian rocks

Greenschist-facies tectonic block, northeast of Fowler Pass fault

Granite: coarse-grained, unfoliated, with 1-2cm quartz phenocrysts

Mafic rocks: chlorite-rich phyllite

Felsic volcanic rocks: foliated muscovite phyllite with 0.1-0.5cm quartz phenocrysts

Amphibolite-facies tectonic block, along upper Tolby Creek

Cross-bedded, aluminous quartzite with hematite, chloritoid, sillimanite; inferred to be part of Ortega Formation of Hondo Group

Upper amphibolite to granulite facies tectonic block

Quartzite: intensely deformed quartzite, locally bedded with thin interlayers of pegmatite and pelitic gneiss

Felsic gneiss: layered quartz-plagioclase-K feldspar metasedimentary gneiss with variable amounts of sillimanite, garnet, biotite, Fe ti oxides

Fine-grained quartzofeldspathic gneiss: relatively homogeneous, weakly foliated, probably metarhyolite

Mafic gneiss: hornblende-plagioclase gneiss, locally may have pyroxene

Granitic gneiss: quartz-plagioclase-K feldspar gneiss with relict granitic textures

Ductile shear zone; dotted where buried beneath Phanerozoic cover, dashed where exposed in float

Depositional or intrusive contact

0 1
km

FIGURE 2. Detailed geologic map of study area showing distribution of rock types. Proterozoic rocks, mapped in detail, are overlain by patches of Late Triassic Dockum Group (Goodknight, 1976) and unconsolidated Quaternary deposits.

Eagle Nest tectonic block

Nearly all rocks in the Eagle Nest tectonic block are intensely folded, foliated, lineated and record a high metamorphic grade. Coarse-grained quartzite crops out near, and is truncated by, the Fowler Pass fault (Fig. 2). Internal folding is common within the quartzite making its thickness difficult to determine, but measurements across one apparently unfolded section give it a minimum thickness near 300 m. The quartzite has thin pelitic interbeds with coexisting sillimanite and microcline. Large kinked books of muscovite, interpreted as retrograde, cut across the dominant foliation and separate sillimanite from K-feldspar in some specimens. Other minerals in pelitic beds include garnet, biotite, plagioclase and accessory ilmenite, magnetite or apatite. Veins of pegmatite up to 10 m thick are interlayered with quartzite, aligned in the plane of foliation and foliated. They contain quartz-K-feldspar-plagioclase ± muscovite. Similar pegmatites are found in most other supracrustal rock types within this block.

Coarse-grained (1–5 mm) quartzofeldspathic gneiss, here termed felsic gneiss, is found south of the Cimarron River along Tolby Creek (Fig. 2). Rocks show parallel compositional layering and foliation; both are folded. Alternating layers rich in plagioclase, K-feldspar or quartz, accompanied by rarer, highly aluminous layers rich in sillimanite and microcline, are interpreted as relict bedding. In many places sillimanite forms knots up to 2 cm across, and locally the sillimanite-K-feldspar assemblages are partially replaced by large books of retrograde muscovite that cut across foliation. A few pelitic beds contain garnet-biotite-sillimanite-plagioclase-microcline-magnetite ± ilmenite, together with a greenish spinel that is a solid-solution between hercynite ($FeAl_2O_4$) and gahnite ($ZnAl_2O_4$; Table 1). Although some green spinels form porphyroblasts, others lie along the edges of magnetite grains and may have been exsolved during cooling. Felsic gneiss contains local segregations 1–3 cm thick and 10–20 cm long, elongate subparallel to foliation, with granitic mineralogy and igneous texture. They are thought to be migmatite produced by in situ partial melting. Most such layers have asymmetric shapes but contain mineral grains that are undeformed or only slightly deformed, suggesting that migmatites were at least partially molten during deformation. Their shapes and orientations indicate that the syntectonic melts may have segregated into shear bands. The felsic gneiss complex represents quartzofeldspathic sedimentary and perhaps rock material heated to temperatures sufficient for partial melting.

A layer of fine-grained, weakly foliated quartzofeldspathic gneiss is exposed in the central part of the map area. Containing plagioclase, quartz, K-feldspar and rare biotite, it is both finer-grained (1–2 mm) and more homogeneous than the felsic gneiss. Although this gneiss bears superficial resemblance to a fine-grained granite, it shows metamorphic microstructures and contains mappable, lensoidal layers of mafic gneiss (Fig. 2). These features suggest that it originated as a stratiform unit.

A large body of granitic gneiss crops out in the southern part of the Eagle Nest tectonic block (Fig. 2). The gneiss is equigranular, poorly to well-foliated and coarse-grained (5–15 mm), composed of plagioclase-K-feldspar-quartz with minor biotite. Thin sections show tabular plagioclase, irregular grain boundaries and myrmekitic textures, suggesting a plutonic origin. Mappable inclusions of mafic rock within granitic gneiss (Fig. 2) contain coarse-grained hornblende-plagioclase-magnetite-K-feldspar. They may represent blocks of wall-rock caught up in the granitic pluton, or they may record mixing of mafic and granitic magmas.

Mafic gneiss is common but not abundant elsewhere in the Eagle Nest tectonic block. Small lenticular bodies lie along the contact between quartzite and felsic gneiss, and along the contact between felsic and granitic gneiss (Fig. 2). More extensive mafic layers crop out within fine-grained quartzofeldspathic gneiss. Most mafic rocks are foliated and lineated, with blue-green hornblende-plagioclase ± quartz ± titanite, an assemblage characteristic of the middle amphibolite facies. Some blue-green hornblende grains have relict cores of the brownish hornblende that is characteristic of the upper amphibolite facies.

TABLE 1. Electron microprobe analyses of Fe-Zn spinels from Eagle Nest tectonic block. Analyzed samples located in Figure 1.

Specimen	88-CIM-76A	89-CIM-192
	Weight percent	
FeO[1]	22.81	12.78
MgO	1.13	0.29
MnO	0.78	0.07
ZnO	17.92	29.88
TiO_2	0.01	0.00
Al_2O_3	57.69	56.83
SiO_2	0.00	0.03
Total	100.34	99.89
	Cations based on 4 oxygens	
Fe	0.56	0.32
Mg	0.05	0.01
Mn	0.02	0.00
Zn	0.39	0.56
Ti	0.00	0.00
Al	1.99	2.00
Si	0.00	0.00

[1]All Fe as FeO

Tolby Meadow tectonic block

Quartzite, the most common lithology in the Tolby Meadow tectonic block, generally exceeds 95 modal percent quartz with accessory titaniferous hematite, rutile and zircon. The quartzite shows bedding outlined by gray streaks, thin aluminous beds and concentrations of mica. Features that may once have been crossbeds are present but none are well-preserved. In most outcrops the quartzite is coarse-grained (0.2–1 mm) and equigranular, with equilibrium metamorphic textures. A few samples collected within 10 m of the contact with the underlying Eagle Nest tectonic block show mylonitic textures, with extreme grain-size reduction and an asymmetric S-C fabric. Pegmatites are absent from this quartzite, in contrast to that in the Eagle Nest tectonic block.

The mineralogy of three samples, all from thin aluminous beds in quartzite of the Tolby Meadow tectonic block, has been studied. One contains chloritoid-muscovite-hematite-quartz whereas the other two have chloritoid-sillimanite-muscovite-hematite-quartz. Sillimanite forms both fibrolitic needles and coarse prisms aligned in the direction of lineation, whereas chloritoid, muscovite and hematite form small, elongate, intensely deformed grains lying in the plane of foliation. All minerals seem to be prograde from their textures. Mineral compositions are given in Table 2. Mineralogy and crossbedding suggest that this quartzite may be part of the Ortega Formation, which is widely exposed in northern New Mexico (Grambling and Williams, 1985; Bauer and

TABLE 2. Electron microprobe analyses of mineral from Tolby Meadow tectonic block. Specimen 88Cim1 located by triangle in Figure 1; specimen TLL-011b collected by T. L. Leyenberger from unspecified location within the tectonic block.

Specimen	TLL-011 b Chloritoid	88-CIM-1 Chloritoid	88-CIM-1 Sillimanite	88-CIM-1 Ti-Hematite
	Weight percent			
FeO[1]	23.66	25.08	0.81	83.12
MgO	1.33	0.96	0.00	0.00
MnO	3.45	2.12	0.00	0.44
ZnO	0.00	0.08	0.00	0.59
TiO_2	0.10	0.02	0.00	8.16
Al_2O_3	40.32	41.21	62.87	0.11
SiO_2	23.62	24.35	37.55	0.01
Total	92.81	93.83	101.23	92.43
X^2_{Fe}	0.80	0.87	- $X_{Fe_2O_3}$	0.85
X^2_{Mg}	0.08	0.06	- X_{FeTiO_3}	0.14
X^2_{Mn}	0.12	0.07	- X_{MnTiO_3}	0.01

[1]All Fe as FeO

[2]$X_i = i/(Fe + Mg + Mn)$

Williams, 1989; Grambling, 1990a, b). U-Pb zircon studies suggest that the Ortega Formation was deposited in the time interval 1700–1690 Ma (S. A. Bowring, oral commun., cited in Grambling, 1986, p. 150).

METAMORPHIC P-T CONDITIONS

Cimarron River tectonic block

Outside the narrow contact-metamorphic aureole surrounding the granitic stock (Figs. 1, 2), mafic rocks have chlorite-albite-epidote-titanite coexisting with an unidentified fibrous mineral. This greenschist assemblage suggests temperatures below 450°C (Fig. 3a). Temperatures were higher within 100 m of the stock, where the assemblage hornblende-plagioclase-chlorite-epidote-quartz indicates 500–550°C. No assemblages constrain the pressure of regional or contact metamorphism.

Eagle Nest tectonic block

Four samples of garnet gneiss from the Eagle Nest tectonic block were analyzed. Garnets were unzoned and nearly pure almandine in one. Other samples had garnets with broad, unzoned cores surrounded by narrow, sharply zoned rims. X_{Fe} and X_{Mn} increased in garnet rims as X_{Mg} fell, a type of zoning characteristic of high-grade metamorphism where intracrystalline diffusion erases growth zoning but imparts retrograde rim zoning (e.g., Grant and Weiblen, 1971; Tracy et al., 1976; Yardley, 1977). Garnet cores were interpreted to preserve compositions stable at the peak of metamorphism, whereas rims were assumed to be retrograde.

Anhedral plagioclase showed homogeneous cores surrounded by zoned, more sodic rims. Cores were assumed to preserve the composition stable at the peak of metamorphism and rims to be retrograde. Rims of pure albite surrounded plagioclase in one specimen (89Cim192) that also contained Na-free microcline. These features probably developed through retrograde exsolution of albite from K-feldspar coupled with overgrowth of the exsolved albite on plagioclase. Feldspars in this sample were not used for barometry.

Biotite compositions were obtained by analyzing 20–30 crystals per sample at 2–5 analyses per crystal. Compositions varied widely in each thin section, with typical specimens showing inversely correlated variations in TiO_2 and Mg/(Mg+Fe), and TiO_2 varying over the range 4 to 2 weight percent. The low-Ti analyses came from parts of biotite grains that contained thin needles of rutile parallel to their (001) cleavage, suggesting that they experienced exsolution of TiO_2. Guidotti (1984) observed that TiO_2 in biotite rises with metamorphic temperature. Applying this logic, peak metamorphic compositions were obtained by averaging compositions of the highest-Ti biotites in a thin section, whereas the retrograde compositions were taken from the lowest-Ti biotites.

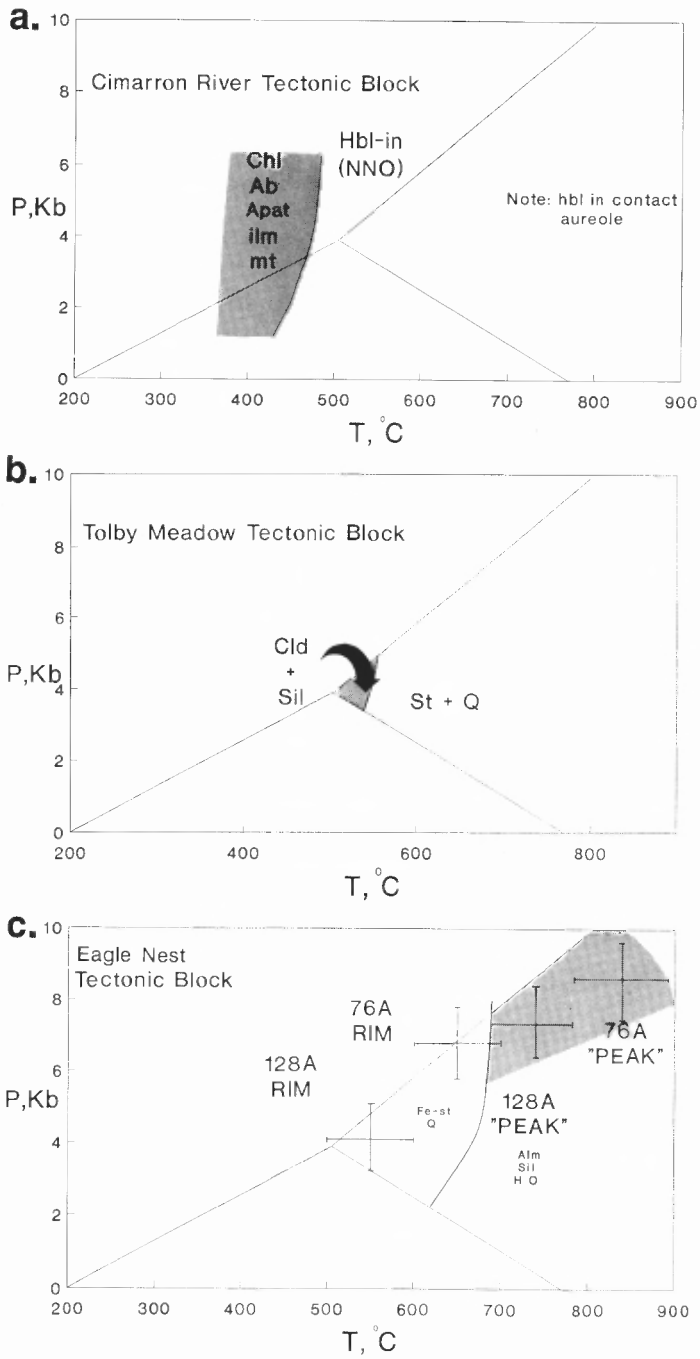


FIGURE 3. Metamorphic P-T conditions derived from Proterozoic rocks in Cimarron Mountains. a, Cimarron River tectonic block. b, Tolby Meadow tectonic block. c, Eagle Nest tectonic block, including both peak and retrograde conditions. P-T estimates derived following procedures described in text. Al_2SiO_5 boundaries from Holdaway (1971); NNO refers to Ni-NiO experimental oxygen buffer.

Resulting peak metamorphic compositions of garnet, biotite and plagioclase are listed in Table 3. They yield P-T estimates shown in Figure 3c: 88Cim76a, 850°C, 8.5 kb; 88Cim128a, 750°C, 7.5 kb; and 89Cim192, 830°C (pressure unspecified). The higher values are considered the most reliable given the propensity for high-temperature minerals to re-equilibrate upon cooling. Garnet and biotite in specimen 88Cim120 had almost no MgO (Table 3) and gave garnet-biotite temperature near 700°C, but this estimate is highly uncertain because of the low MgO.

Because garnet in specimen 88Cim120 was essentially pure almandine and coexisted with sillimanite, it sets an independent limit on temperature: 700°C is the minimum needed to obtain coexisting almandine and sillimanite (Richardson, 1968; Dutrow and Holdaway, 1989). Thus, all P-T estimates place the peak of metamorphism above 700°C, in the granulite facies.

Inferred retrograde mineral compositions are also listed in Table 3. They yield apparent P-T estimates as follows: 88Cim76a, 650°C, 6.8 kb; 88Cim128a, 550°C, 3.8 kb; and 89Cim192, 560°C (pressure unknown). Retrograde conditions taken together with peak conditions define an apparent P-T path falling from 830°C, 8 kb toward the Al_2SiO_5 triple point (Fig. 3c).

Tolby Meadow tectonic block

The coexistence of chloritoid with sillimanite (Table 2) constrains metamorphic conditions in the Tolby Meadow tectonic block. These two minerals can coexist only in a narrow range of P-T conditions near the kyanite-andalusite-sillimanite triple point, at 3.5–4.5 kb, 500–530°C (Fig. 3b).

STRUCTURES SEPARATING THE TECTONIC BLOCKS

Eagle Nest and Tolby Meadow blocks

The contact between the Eagle Nest and Tolby Meadow tectonic blocks crops out in the southwestern part of the study area (Figs. 1, 2). The Tolby Meadow tectonic block physically overlies the Eagle Nest tectonic block, best seen in the steep cliff exposures north of Tolby Meadow. Elsewhere the contact dips beneath the Tolby Meadow block indicating the same geometry. The irregular nature of that contact (Fig. 2) is interpreted as a consequence of folding, because bedding and foliation planes are folded along with the contact. However, the contact has a subhorizontal enveloping surface, suggesting that it was nearly flat prior to the folding.

Both tectonic blocks preserve textural evidence their juxtaposition. All rocks show foliation and lineation defined by aligned micas, FeTi oxides, hornblende and/or sillimanite. Foliation trends are variable (Fig. 2), but mineral elongation lineations cluster about a northwest-southeast trend. Asymmetries shown by grains of sillimanite, muscovite and titaniferous hematite, foliations interpreted as recrystallized S-C surfaces, and apparent melt-filled shear bands in migmatite record top-to-the-southeast movement. Recrystallization has annealed the finer details of these textures in many rocks, consistent with the interpretation that the deformation took place at metamorphic temperatures. Fresh mylonite fabrics found in a few samples from the block boundary may indicate that some motion took place as temperatures fell below that at which the two blocks were first joined.

Cimarron River and Eagle Nest blocks

The high-angle Fowler Pass fault separates the Cimarron River and Eagle Nest tectonic blocks (Fig. 1). Greenschist-facies metarhyolite of the former tectonic block shows a weak northwesterly foliation 150 m from the fault. The foliation, defined by flattened quartz phenocrysts and aligned sericite, parallels the fault at N50°W, 90°. Two thin layers of foliated and lineated banded ironstone crop out 100 m from the fault; layering, foliation and lineation all lie parallel to the fault. Metarhyolite near the banded ironstone has subvertical foliation and subhorizontal lineation, with asymmetric quartz porphyroclasts (phenocrysts) having recrystallized quartz tails that record right-lateral, strike-slip shear. Foliation and lineation become progressively more intense toward the fault. Within 10–20 m of it, metarhyolite grades into a streaky, fine-grained rock that lacks visible quartz porphyroclasts but has extremely well-developed subhorizontal lineation and subvertical foliation.

Within 1 km southwest of the Fowler Pass fault, granulite-facies rocks of the Eagle Nest tectonic block are folded with axial planes subparallel to the fault. Mylonitic high-grade quartzite has partially annealed to well-preserved quartz ribbons, and coarse, asymmetric muscovite porphyroclasts are elongated parallel to the trace of the fault.

The ductile deformational textures found on both sides of the Fowler Pass fault are interpreted to record the joining of the Eagle Nest and Cimarron River tectonic blocks. An important observation is that the fabrics are defined by retrograde minerals in the high-grade rocks but by apparent prograde minerals in the low-grade rocks.

Brittle deformation is superimposed on these ductile fabrics. Goodknight (1976) and Wobus (1989) noted that flat-lying sedimentary rocks of the Late Triassic Dockum Group are found at different elevations across the Fowler Pass fault, concluding that this indicated vertical post-Triassic slip.

$^{40}AR/^{39}AR$ GEOCHRONOLOGY

Three mineral concentrates prepared from a preliminary sample suite have been analyzed by the $^{40}Ar/^{39}Ar$ incremental release technique.

TABLE 3. Peak (core) and retrograde (rim) mineral compositions in four specimens from Eagle Nest tectonic block, together with inferred metamorphic P-T conditions.

Specimen	88-CIM-120			88-CIM-76A									88-CIM-128A									89-CIM-192					
	Grt Pk	Bt Pk	Ms R	Grt Pk	Grt R	Bt Pk	Bt R	Pl Pk	Pl R	Sil	Ms R	Ilm	Grt Pk	Grt R	Bt Pk	Bt R	Pl Pk	Pl R	Sil	Ms R	Ilm	Grt Pk	Grt R	Bt Pk	Bt R	Pt Pk	Ilm[2] (wx)
	Weight percent																										
FeO[1]	43.25	29.68	2.12	32.05	31.71	24.92	22.90	0.00	0.21	0.64	3.04	43.91	29.00	29.05	23.06	20.84	0.02	1.00	0.46	2.85	43.39	38.66	38.83	28.33	27.69	0.00	38.24
MgO	0.23	0.73	0.05	1.84	1.15	5.19	5.01	-	-	0.00	0.36	0.05	1.95	1.38	7.39	8.59	-	-	0.00	0.48	0.01	0.74	0.51	1.99	2.63	-	0.02
MnO	0.22	0.00	0.00	8.22	9.51	0.29	0.23	-	-	0.01	0.05	2.52	8.40	10.07	0.20	0.14	-	-	0.00	0.00	5.72	2.28	3.03	0.09	0.13	-	1.37
CaO	0.26	0.03	0.00	1.27	1.27	0.09	0.11	5.99	3.99	0.00	0.03	-	1.89	2.06	0.00	0.02	7.59	5.89	-	0.00	-	1.07	1.04	0.02	0.07	4.18	-
TiO_2	0.05	1.89	0.16	0.00	0.02	3.31	2.50	-	-	0.03	0.65	50.96	0.00	0.05	2.95	2.27	-	-	0.00	0.81	49.89	0.01	0.00	3.89	2.92	-	53.97
Al_2O_3	20.52	21.74	37.07	21.00	20.65	19.25	20.58	25.17	23.98	61.15	35.18	-	21.07	20.58	19.46	20.11	26.51	26.33	61.67	36.10	-	20.78	21.36	19.84	18.88	24.12	0.01
SiO_2	36.59	32.60	44.93	37.59	37.33	33.93	35.20	60.18	62.74	36.57	45.44	-	37.60	37.12	34.66	36.45	59.37	58.60	36.60	45.91	-	36.66	36.55	32.41	34.21	63.34	0.01
K_2O	-	8.87	9.08	-	-	9.22	8.27	0.06	0.10	-	10.80	-	-	-	9.65	9.77	0.10	0.94	-	9.99	-	-	-	9.66	9.26	0.14	-
Na_2O	-	0.13	1.67	-	-	0.12	0.10	8.39	9.25	-	0.37	-	-	-	0.06	0.04	7.25	6.97	-	0.52	-	-	-	0.03	0.04	9.57	-
Total	101.11	95.67	95.06	101.97	101.64	96.33	94.90	99.79	100.27	98.50	95.92	97.44	99.91	100.31	97.43	97.23	100.84	99.63	98.74	96.66	99.13	100.20	101.32	96.25	95.83	101.36	94.21
Peak P-T (Pk)		>700°C		850°C, 8.5 kb									750°C, 7.5 kb									830°C					
Retrograde P-T (R)				650°C, 6.8 kb									550°C, 3.8 kb									560°C					

[1]Total Fe as FeO

[2]Ilmenite was weathered/altered; analytical total includes 0.58 wt% ZnO

Hornblende

Concentrates from two samples (88Cim155, 88Cim159) showed variations in apparent ages of gas fractions evolved at low and high experimental temperatures, matched by some fluctuation in apparent K/Ca ratios (Figs. 4, 5). Results suggest argon loss from compositionally distinct and variably retentive phases such as: (1) optically undetectable traces of mineral contaminants in the concentrates; (2) minor exsolution or compositional zonation within amphibole; (3) trace chlorite replacement of amphibole; or (4) intracrystalline inclusions. In general, over 75% of the total ^{39}Ar released from each concentrate shows similar K/Ca, indicating evolution of this gas from compositionally uniform amphibole grains.

Intermediate-temperature gas fractions evolved from sample 88Cim159 record apparent $^{40}Ar/^{39}Ar$ ages that correspond to a plateau of 1401 ± 2 Ma (Fig. 4a). The plateau data yield an isotope correlation ($^{36}Ar/^{40}Ar$ vs. $^{39}Ar/^{40}Ar$; MSWD = 1.67) with inverse ordinate intercept ($^{40}Ar/^{36}Ar$) of 316.7 ± 19.3 and age of 1397 ± 4 Ma. The inverse ordinate intercept is similar to the $^{40}Ar/^{36}Ar$ ratio of the present-day atmosphere, suggesting little or no intracrystalline extraneous argon. The 1401 ± 2 Ma age is considered geologically significant, interpreted as the last cooling through temperatures required for intracrystalline retention of argon.

The hornblende concentrate from sample 88Cim155 displays an internally discordant age spectrum (Fig. 5a). Intermediate-temperature gas fractions show similar apparent K/Ca ratios but fail to define a plateau. However, intermediate and high-temperature gas fractions yield a well-defined isotope correlation (MSWD = 1.52) with an age of 1394 ± 8 Ma and an inverse ordinate intercept of 454 ± 14, indicative of slight intracrystalline contamination with extraneous argon of relatively uniform composition. The isotope correlation age is considered geologically reliable.

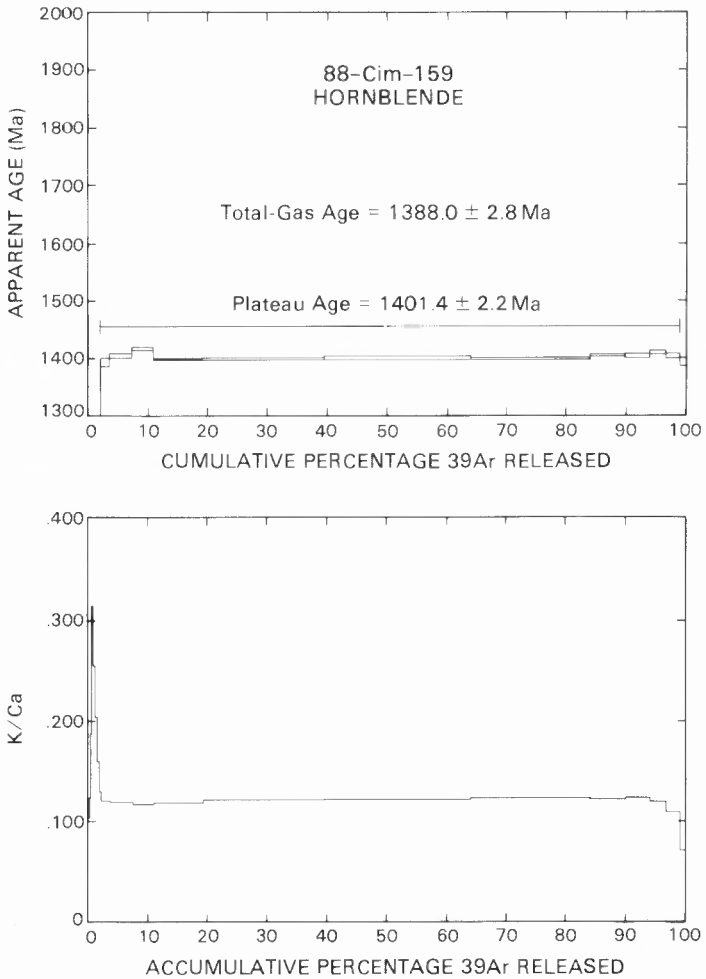


FIGURE 4. Argon isotopic data from hornblende separate 88Cim159. Apparent age plotted against cumulative amount of argon released, with apparent plateau at 1401 ± 2 Ma (above). Apparent K/Ca ratios remain constant between 5% and 95% of gas released (below).

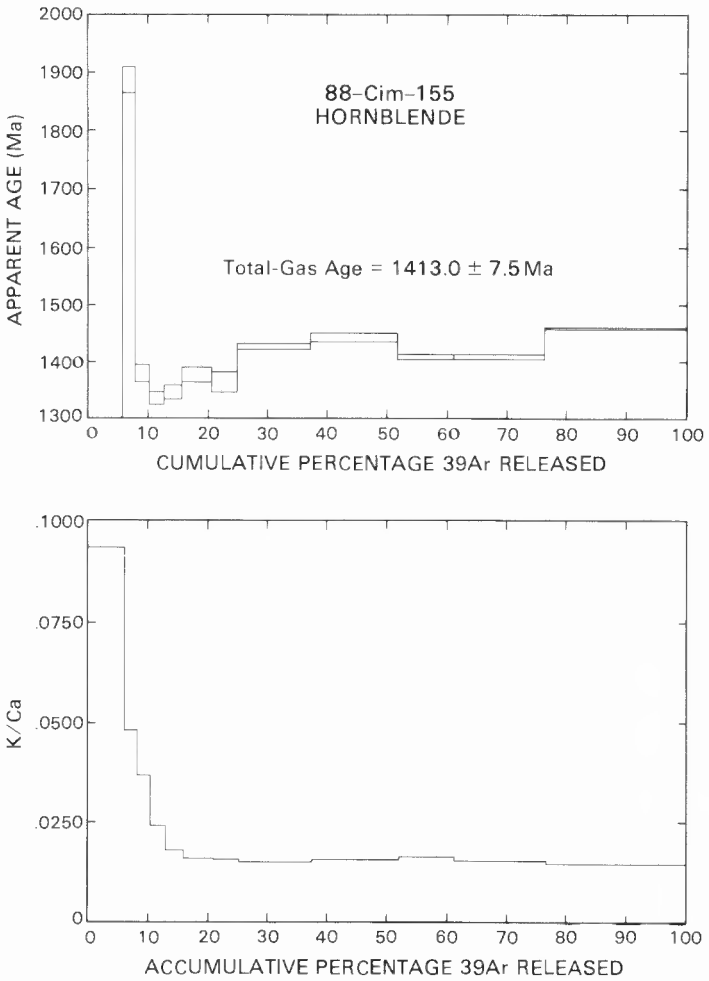


FIGURE 5. Argon isotopic data from hornblende separate 88Cim155. Apparent age plotted against cumulative amount of gas released (above). Data fail to define plateau. Apparent K/Ca ratios remain constant between 20 and 100% of gas released (below). Analyses from intermediate and high-temperature gas fractions give isotope correlation indicating age of 1394 ± 8 Ma.

Muscovite

Apparent K/Ca ratios recorded by increments evolved from muscovite (88Cim134) are large with considerable associated uncertainties, but they show no significant or systematic variations throughout the analysis except in the small-volume increment evolved at the lowest experimental temperature (which yields an apparent age of 770 Ma; Fig. 6). This increment likely records at least some gas evolved from a nonrefractory mineral contaminant.

The remainder of the muscovite age spectrum is internally discordant (Fig. 6), with apparent ages increasing markedly from near 1100 Ma to 1255 ± 4 Ma. Apparent $^{40}Ar/^{39}Ar$ ages continue to increase but less markedly throughout the remaining gas increments, from 1269 ± 2 Ma to 1294 ± 4 Ma. Therefore, the data do not rigorously define a plateau. The consistent apparent K/Ca ratios of all but the first gas increment indicate that the variation in apparent ages reflects a natural intracrystalline gradient in the concentration of ^{40}Ar.

The character of spectra discordance is identical to that predicted by Turner (1968) to develop as a result of partial diffusive loss of radiogenic ^{40}Ar during a thermal event superimposed on the one in which muscovite initially grew. Similar behavior has been noted for thermally overprinted

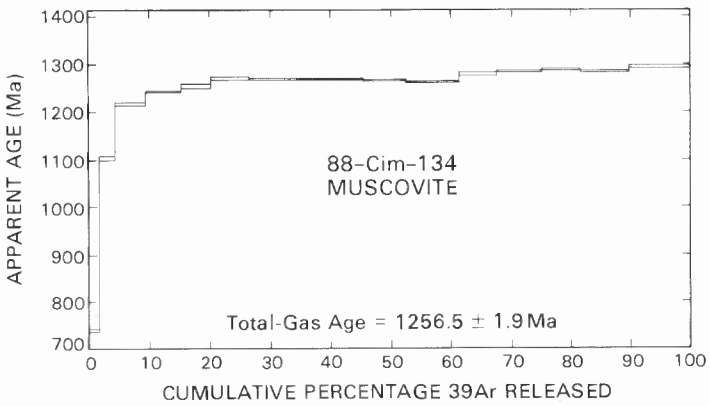


FIGURE 6. Summary of argon isotopic data from muscovite separate 88Cim134. Interpretation summarized in text.

muscovite by numerous workers including Snee et al. (1988) and Dallmeyer and LeCorche (1989). Comparison of the spectrum with the theoretical spectra of Turner (1968) suggests that the muscovite also experienced slight (less than 10%) loss of argon in a low-grade thermal overprint no older than 1100 Ma, the approximate age of the lowest-temperature increment with normal K/Ca ratio.

DISCUSSION

Ductile shear zones divide Proterozoic rocks of the Cimarron Mountains into the Cimarron River, Eagle Nest and Tolby Meadow tectonic blocks. The Fowler Pass fault separates the first two tectonic blocks, whereas the subhorizontal shear zone separates the second tectonic block from the third. The three tectonic blocks preserve distinct differences in their peak metamorphic grade (Fig. 3): greenschist facies in the Cimarron River tectonic block, lower amphibolite facies in the Tolby Meadow tectonic block and granulite facies in the Eagle Nest tectonic block.

Rock types

The Cimarron River block contains by far the highest proportion of mafic rocks of the three tectonic blocks. Wobus (1989) presented major-element chemical analyses of several metavolcanic rocks from this tectonic block. His data permit that protoliths were basalt for mafic metavolcanic rocks and rhyolite for felsic metavolcanic rocks, with plutonic rocks defining a calc-alkaline differentiation trend. This interpretation should be treated with caution as it is based upon mobile elements such as K_2O. He also suggested that the rocks initially formed at a time near 1750 Ma, by drawing analogies to dated rocks in the Taos Range. No U-Pb zircon dates are available from the Cimarron Mountains, and U-Pb zircon ages from metavolcanic rocks across New Mexico range from 1765 Ma to 1650 Ma (Bowring et al., 1983; Reed, 1984; Robertson et al., 1991). Until the structural relationships among Proterozoic tectonic blocks in New Mexico are better understood, we hesitate to endorse Wobus's age assignment.

Wobus (1989) treated all rocks but quartzite from the area of the Eagle Nest tectonic block as plutonic, identifying the quartzofeldspathic rocks as granite and the mafic rocks as gabbro. He suggested that the metagabbro had higher Al_2O_3 and lower Fe(total) than mafic rocks in the Cimarron River tectonic block. However, the Eagle Nest tectonic block contains many rocks with sedimentary and volcanic protoliths; plutonic rocks are confined to its southern part (Fig. 1). Because Wobus (1989) did not publish sample locations, it is possible that his analyzed samples came from supracrustal rocks.

Wobus (1989) assumed that quartzite found near the Fowler Pass fault was the same as that found in Tolby Meadow (Fig. 2). However, mineral assemblages show that the former quartzite was heated in excess of 700°C, whereas the latter never exceeded 530°C. The two quartzites might be different parts of a single stratigraphic layer subjected to different metamorphic histories, but we suspect them to be different stratigraphic units.

Deformation and metamorphism

The Eagle Nest and Tolby Meadow tectonic blocks are separated by a subhorizontal ductile shear zone, with the Eagle Nest block beneath the shear zone and the Tolby Meadow block above it. Mineral lineations and asymmetries preserved above, within and below the shear zone show top-to-the-southeast movement, which we interpret to be related to joining of the two tectonic blocks. Granulite-facies minerals in the Eagle Nest tectonic block formed at crustal depths of 25–30 km, and their apparent retrograde P-T path (Fig. 3c) shows cooling and decompression on a trajectory that intersects the peak P-T conditions of the Tolby Meadow tectonic block (Fig. 3b). We infer the pressure of the intersection (4 kb) to represent the depth (14 km) at which the two tectonic blocks became joined.

The P-T path of the granulites indicates upward movement in excess of 10 km, presumably during the event that juxtaposed the two tectonic blocks. This value places a minimum limit on the offset recorded by the subhorizontal shear zone, based on the premise that particle motion trajectories in rocks below the shear zone were vertical. Given that the shear fabrics indicate subhorizontal motion, total offset must have exceeded 10 km. If one arbitrarily assumes that the lower-crustal rocks moved upward at an angle of 5° to the horizontal, then offset across the shear zone exceeded 100 km.

Textures along the steep, northwest-trending Fowler Pass fault suggest that dextral strike-slip shear juxtaposed the Cimarron River and Eagle Nest tectonic blocks (Figs. 1, 2). The ductile nature of deformation, the lack of prograde or retrograde changes in mineralogy of greenschist-facies rocks near the fault, and the retrogression of granulites near the fault indicate that the two tectonic blocks were juxtaposed when metamorphic conditions were in the greenschist facies.

The subhorizontal shear zone and the Fowler Pass fault do not cut one another in outcrop. Nevertheless, differences in metamorphic grade of the two shear zones lead us to believe that the Fowler Pass fault is the younger.

Dating the tectonic assembly

Harrison (1981) indicated that rates of argon diffusion in hornblende are little affected by composition, with closure temperatures of 500 ± 25°C characterizing the most likely metamorphic cooling rates. In contrast, argon closure temperature for muscovite has not been determined rigorously. Preliminary data of Robbins (1972) used in the diffusion equations of Dodson (1973) suggest closure temperatures near 375–400°C, but comparison of partially rejuvenated muscovite argon systems with overprint temperatures estimated from fluid inclusions (Snee et al., 1988) indicates that closure temperatures could be as low as 270–285°C in very slowly cooled metamorphic terranes. These data can be used to place constraints upon the timing of Proterozoic tectonic events in the Cimarron Mountains.

Because the closure temperatures for argon diffusion in hornblende lie close to that at which the Tolby Meadow and Eagle Nest tectonic blocks were joined (Fig. 3), it seems likely that the two hornblende ages, 1394 ± 8 and 1401 ± 2 Ma, date this stage of the tectonic assembly of the Cimarron Mountains. Although cooling at rates considerably below 5°C/Ma might invalidate this interpretation, unusually slow cooling is inconsistent with argon isotopic data obtained from Proterozoic rocks elsewhere in New Mexico. For example, hornblende and muscovite $^{40}Ar/^{39}Ar$ ages near Albuquerque are nearly concordant at 1395–1420 Ma, and hornblende ages in the Manzano Mountains south of Albuquerque fall in the range 1420–1440 Ma, with muscovite reset by a younger thermal and tectonic event at 1350 Ma (Grambling et al., unpubl., 1990; Thompson et al., unpubl., 1990).

Muscovite argon data from the Cimarron Mountains are difficult to interpret, largely due to the small data base. The one spectrum appears not to reflect assembly of the Eagle Nest and Tolby Meadow blocks. Instead, it seems to record a younger thermal event near 1295 Ma at a temperature sufficient to nearly resent muscovite, overprinted by a low-temperature thermal event near 1100 Ma. The significance of these events is unclear: either may date the assembly of the Cimarron River and Eagle Nest tectonic blocks across the Fowler Pass fault. That fault

is oriented nearly perpendicular to the Grenville front, which extends northeast from southern New Mexico and central Texas to northeastern Canada. If the muscovite spectrum does record movement on the fault, then it may be a consequence of the Grenville Orogeny, perhaps a Grenville "escape fault" (Tapponier et al., 1982).

CONCLUSIONS

The portion of the Cimarron Mountains examined in this study covers only 25 km^2 (Fig. 1), yet Proterozoic rocks record a complex geologic history. They outline three crustal blocks metamorphosed at contrasting temperatures and depths, probably in separate geographic localities. The three blocks were assembled into their present geometry by two major ductile shear zones.

The highest-grade rocks, granulites in the Eagle Nest tectonic block, underwent peak metamorphism at 800–850°C, 7.5–8.5 kb, followed by retrograde cooling and decompression on a trajectory toward the Al_2SiO_5 triple point. The Tolby Meadow tectonic block, with peak metamorphic conditions near the Al_2SiO_5 triple point, overlies the Eagle Nest tectonic block, separated from it by a subhorizontal ductile shear zone. The Tolby Meadow block preserves no record of its P-T path, although its peak conditions (500–530°C, 3.5–4.5 kb) coincide with retrograde conditions of the granulites. We suggest that ductile crustal extension joined these two tectonic blocks at 1400 Ma.

The peak P-T conditions and the inferred retrograde path of the Eagle Nest tectonic block are similar to those shown by high-grade gneiss in the Taos Range, 50–80 km northwest of the Cimarron Mountains (Grambling et al., 1989). There, a subhorizontal, top-to-the-southeast ductile shear zone separates underlying granulite-facies gneiss from overlying Al_2SiO_5 triple-point quartzite, just as in the Cimarron Mountains. Given that similar ductile shear zones separate rocks with similar differences in metamorphic grade, it seems plausible that the two areas expose different parts of a vast, flat-lying, mid-crustal deformation zone. If this speculation is correct, then the subhorizontal shear zone covers at least 10,000 km^2.

Grambling (1986) and Grambling et al. (1989) reported peak metamorphism near the Al_2SiO_5 triple point across large parts of northern and central New Mexico. Hornblende $^{40}Ar/^{39}Ar$ ages in this 75,000 km^2 area fall in the range 1440–1395 Ma (this study; Thompson et al., unpubl., 1990; Grambling et al., unpubl., 1990). Preliminary studies using the Gibbs method suggest that the whole area saw a metamorphic P-T path of slight cooling during decompression, passing from the stability field of kyanite to sillimanite to andalusite (Daniel et al., unpubl., 1990). This P-T path lies at lower P and T but otherwise is similar to that shown in Figure 3c. Crustal extension may have formed this P-T path in the upper parts of the continental crust, at the same time that the lower crust was thinning and cooling along the path shown in Figure 3c. Tectonic contacts separating amphibolite-facies rocks from buried granulite-facies rocks may underlie Al_2SiO_5 triple-point rocks across much of northern and central New Mexico.

North-verging ductile thrusts that preceded the peak of Proterozoic metamorphism are well-documented in northern New Mexico (cf. Robertson et al., 1991). Although no such thrusts were found in the Cimarron Mountains, it seems reasonable that they thickened the crust prior to the 1400 Ma crustal thinning event reported here.

ACKNOWLEDGMENTS

Grambling thanks the staff of the New Mexico Bureau of Mines and Mineral Resources for their encouragement and support. Research expenses were funded by the New Mexico Bureau of Mines and Mineral Resources and National Science Foundation Grant EAR-8816402. The electron microprobe used to obtain mineral analyses was funded in part by NSF Grant EAR-8201211. Paul Bauer, Chris Mawer, Jane Pedrick and Chris White provided helpful review of this manuscript, and George Conrad kept the JEOL 733 electron microprobe in superb condition.

REFERENCES

Alexander, E. C., Jr., Michelson, G. M. and Lanphere, M. A., 1978, MMhb-1. A new $^{40}Ar/^{39}Ar$ dating standard; *in* Zartman, R. E., ed., Short papers of the Fourth International Conference, geochronology, cosmochronology, isotope geology: U.S. Geological Survey, Open-file Report 78-701, pp. 6–8.

Apted, M. J. and Liou, J. G., 1983, Phase relations among greenschist, epidote amphibolite, and amphibolite in a basaltic system: American Journal of Science, v. 283-A, pp. 328–354.

Bauer, P. W. and Williams, M. L., 1989, Stratigraphic nomenclature of Proterozoic rocks, northern New Mexico—revisions, redefinitions, and formalization: New Mexico Geology, v. 11, pp. 45–52.

Bowring, S. A., Kent, S. C. and Summer, W., 1983, Geology and U-Pb geochronology of Proterozoic rocks in the vicinity of Socorro, New Mexico: New Mexico Geological Society, Guidebook 34, pp. 137–142.

Dallmeyer, R. D. and Keppie, J. D., 1987, Polyphase late Paleozoic tectonothermal evolution of the southwestern Meguma Terrane, Nova Scotia: Evidence from $^{40}Ar/^{39}Ar$ mineral ages: Canadian Journal of Earth Sciences, v. 24, pp. 1242–1254.

Dallmeyer, R. D. and LeCorche, J. P., 1989, $^{40}Ar/^{39}Ar$ polyorogenic mineral age record within the central Mauritanide orogen, West Africa: Geological Society of America Bulletin, v. 101, pp. 55–70.

Dalrymple, G. B, Alexander, E. C., Lanphere, M. A. and Kraker, G. P., 1981, Irradiation of samples for $^{40}Ar/^{39}Ar$ dating using the Geological Survey TRIGA reactor: U.S. Geological Survey, Professional Paper 1176, 55 pp.

Dodson, M. H., 1973, Closure temperature in cooling geochronological and petrological systems: Contributions to Mineralogy and Petrology, v. 40, pp. 259–274.

Dutrow, B. L. and Holdaway, M. J., 1989, Experimental determination of the upper thermal stability of Fe-staurolite + quartz at medium pressures: Journal of Petrology, v. 30, pp. 229–248.

Ganguly, J. and Saxena, S. K., 1984, Mixing properties of aluminosilicate garnets: constraints from natural and experimental data, and applications to geothermo-barometry: American Mineralogist, v. 69, pp. 88–97.

Goodknight, C. S., 1976, Cenozoic structural geology of the central Cimarron Range, New Mexico: New Mexico Geological Society, Guidebook 27, pp. 137–140.

Grambling, J. A., 1986, A regional gradient in the composition of metamorphic fluids in pelitic schist, Pecos Baldy, New Mexico: Contributions to Mineralogy and Petrology, v. 94, pp. 149–164.

Grambling, J. A., 1988, A summary of Proterozoic metamorphism in northern and central New Mexico: the regional development of 520°C;, 4-kb rocks; *in* Ernst, W. G., ed., Metamorphism and crustal evolution of the western United States: Rubey volume VII, Prentice-Hall, pp. 447–465.

Grambling, J. A., 1990a, Proterozoic geology of the Rincon Range north of Guadalupita, New Mexico: New Mexico Geological Society, Guidebook 41.

Grambling, J. A., 1990b, Proterozoic metamorphic rocks near Comanche Point, New Mexico: New Mexico Geological Society, Guidebook 41.

Grambling, J. A. and Codding, D. B., 1982, Stratigraphic and structural relationships of multiply deformed Precambrian metamorphic rocks in the Rio Mora area, New Mexico: Geological Society of America Bulletin, v. 93, pp. 127–137.

Grambling, J. A. and Williams, M. L., 1985, The effects of Fe^{3+} and Mn^{3+} on aluminum silicate phase relations in north-central New Mexico, U.S.A.: Journal of Petrology, v. 26, pp. 324–354.

Grambling, J. A., Williams, M. L., Smith, R. F. and Mawer, C. K., 1989, The role of crustal extension in the metamorphism of Proterozoic rocks in New Mexico: Geological Society of America, Special Paper 235, pp. 87–110.

Grant, J. A. and Weiblen, P. W., 1971, Retrograde zoning in garnet near the second sillimanite isograd: American Journal of Science, v. 270, pp. 281–296.

Guidotti, C. V., 1984, Micas in metamorphic rocks; *in* Bailey, S. W., ed., Micas: Reviews in Mineralogy, v. 13, pp. 357–468.

Hackler, R. T. and Wood, B. J., 1989, Experimental determination of Fe and Mg exchange between garnet and olivine and estimation of Fe-Mg mixing properties in garnet: American Mineralogist, v. 74, pp. 994–999.

Harrison, T. M., 1981, Diffusion of ^{40}Ar in hornblende: Contributions to Mineralogy and Petrology, v. 78, pp. 324–331.

Harrison, T. M. and FitzGerald, J. D., 1986, Exsolution in hornblende and its consequences for $^{40}Ar/^{39}Ar$ age spectra and closure temperature: Geochimica et Cosmochimica Acta, v. 50, pp. 247–253.

Holdaway, M. J., 1971, Stability of andalusite and the aluminum silicate phase diagram: American Journal of Science, v. 271, pp. 97–131.

Koziol, A. M. and Newton, R. C., 1988, Redetermination of the anorthite breakdown reaction and improvement of the plagioclase-garnet-Al_2SiO_5-quartz geobarometer: American Mineralogist, v. 73, pp. 216–223.

Mawer, C. K., Grambling, J. A., Williams, M. L., Bauer, P. W. and Robertson, J. M., 1990, The relationship of the Proterozoic Hondo Group to older rocks, southern Picuris Mountains and vicinity, northern New Mexico: New Mexico Geological Society, Guidebook 41.

Moody, J. B., Meyer, D. and Jenkins, J. E., 1983, Experimental characterization of the greenschist/amphibolite boundary in mafic systems: American Journal of Science, v. 283, pp. 48–96.

Newton, R. C. and Haselton, H. T., 1981, Thermodynamics of garnet plagioclase-Al_2SiO_5 geobarometer; *in* Newton, R. C. et al., Thermodynamics of minerals and melts: Advances in Physical Geochemistry, v. 1, pp. 131–148.

Rao, B. B. and Johannes, W., 1979, Further data on the stability of staurolite + quartz and related assemblages: Neues Jahrbuch für Mineralogie Monatschefte, pp. 437–447.

Reed, J. C., Jr., 1984, Proterozoic rocks of the Taos Range, Sangre de Cristo Mountains, New Mexico: New Mexico Geological Society, Guidebook 35, pp. 179–186.

Richardson, S. W., 1968, Staurolite stability in a part of the system Fe-Al-Si-O-H: Journal of Petrology, v. 9, pp. 467–488.

Robbins, G. A., 1972, Radiogenic argon diffusion in muscovite under hydrothermal conditions [M.S. thesis]: Providence, Brown University, 23 pp.

Robertson, J. M., Grambling, J. A., Mawer, C. K., Bowring, S. A., Williams, M. L., Bauer, P. W. and Silver, L. A., 1991, Precambrian of New Mexico: Decade of North American Geology, v. C-2, in press.

Snee, L. W., Sutter, J. F. and Kelly, E. C., 1988, Thermochronology of economic mineral deposits: Dating stages of mineralization at Panasqueira, Portugal, by high-precision $^{40}Ar/^{39}Ar$ age-spectrum techniques on muscovite: Economic Geology, v. 83, pp. 335–354.

Steiger, R. H. and Jäger, E., 1977, Subcommission on geochronology: convention on the use of decay constants in geo- and cosmochronology: Earth and Planetary Sciences, v. 36, pp. 359–362.

Tapponier, P., Peltzer, G., LeDain, A. Y., Armijo, R. and Cobbold, P. R., 1982, Propagating extrusion tectonics in Asia: new insights from simple experiments with plasticine: Geology, v. 10, pp. 611–616.

Tracy, R. J., Robinson, P. and Thompson, A. B., 1976, Garnet composition and zoning in the determination of temperature and pressure of metamorphism, central Massachusetts: American Mineralogist, v. 61, pp. 762–775.

Turner, G., 1968, The distribution of potassium and argon in chondrites; *in* Ahrens, L. H., ed., Origin and distribution of the elements: New York, Pergamon Press, pp. 378–398.

Williams, M. L. and Grambling, J. A., 1990, Manganese, ferric iron, and the equilibrium between garnet and biotite: American Mineralogist, in press.

Wobus, R. A., 1989, Proterozoic supracrustal rocks and plutons of the Cimarron Canyon area, north-central New Mexico: Geological Society of America, Special Paper 235, pp. 111–118.

Yardley, B. W. D., 1977, An empirical study of diffusion in garnet: American Mineralogist, v. 62, pp. 793–800.

York, D., 1969, Least squares fitting of a straight line with correlated errors: Earth and Planetary Science Letters, v. 5, pp. 320–324.



An unusual photograph of the interior of the Carrington Store in Elizabethtown around 1900. Retail prices in such a store were: flour, $10 per hundred; coffee, $.65 per lb; sugar, $.45 per lb; bacon, $.45 per lb; vinegar, $1 per pint; beef, $.15 per lb; corn, $.07 per lb; oats, $.06 per lb; and molasses, $5 per gal. Courtesy of Kit Carson Foundation.